Monthly Notices of the ROYAL ASTRONOMICAL SOCIETY

Mon. Not. R. Astron. Soc. **407,** 2599–2610 (2010) doi:10.1111/j.1365-2966.2010.17095.x

An unbiased pilot survey for Galactic water masers

J. L. Caswell[1]★ and S. L. Breen[1,2]

[1]*Australia Telescope National Facility, CSIRO, PO Box 76, Epping, NSW 2121, Australia*
[2]*School of Mathematics and Physics, University of Tasmania, Private Bag 37, Hobart, Tasmania 7001, Australia*

Accepted 2010 May 26. Received 2010 May 26; in original form 2010 May 4

ABSTRACT

The Australia Telescope Compact Array has been used in a fast surveying mode to study the 22-GHz transition of water in two small sample regions of the southern Galactic plane. The observations allow an unbiased search for water masers, including any that may have no association with masers from other molecules (or indeed, no association with any other detectable celestial object). Positions with arcsecond accuracy were obtained from the original survey data for detected sources, and these were re-observed at an epoch more than two years later. Variability of the spectra between the epochs was considerable: our total of 32 masers comprises 24 detected at both epochs, two detected at only the first epoch and six detected at only the follow-up epoch. The success of our surveying mode shows it to be a practical strategy for the difficult task of extending unbiased water maser surveys to a large portion of the Galactic plane. Our results show quantitatively the effect of variability on the completeness of surveys conducted at a single epoch.

Most of our maser detections are new discoveries. Only four had previously been detected (in searches towards interesting targets in the survey area). The high density of water masers from our unbiased survey supports earlier suggestions that they are the most populous maser species, and one of the most sensitive and reliable tracers of massive young stellar objects – newly forming massive young stars. The spectra of nine masers show high-velocity emission, and they show a striking preponderance of blueshifted high-velocity features. This is compatible with such blueshifts being a characteristic of populations dominated by masers at the earliest evolutionary stage of star formation, in some cases prior to the onset of methanol masers. Amongst the high-velocity emission sources there are two new examples where blueshifted high-velocity outflows dominate the total emission; these substantially increase the previously known meagre population of five such objects and suggest that they may be surprisingly abundant.

Key words: masers – surveys – stars: formation – ISM: molecules.

1 INTRODUCTION

Water masers are the most populous maser species in our Galaxy. This inference is based not on large surveys, but indirectly from the combination of detections towards various targeted objects, and many serendipitous discoveries while observing the intended targets (Caswell 2007). Two major varieties of water maser exist – those in the envelopes of evolved asymptotic giant branch stars and those in the envelopes of young stellar objects (YSOs), the most powerful being those associated with the more massive YSOs, newly forming young massive stars (Palagi et al. 1993; Furuya et al. 2003).

Massive YSOs account for the majority of strong OH masers in the 1665-, 1667- and 6035-MHz transitions, and perhaps all of the ubiquitous 6668-MHz methanol masers (Minier et al. 2003). They may account for the bulk of 22-GHz water masers in a sensitivity-limited survey of the Galactic disc. At each maser site of this variety, there are typically many maser spots residing in a dusty molecular envelope around the newly forming massive star. Precise comparison of the maser spot distributions of OH, methanol and water (Forster & Caswell 1989, 1999; Caswell 1997) establish that all three species are commonly intermingled, over similar total extents, and usually confined within a diameter of less than 30 mpc. Slightly larger sizes may occur amongst water masers exhibiting outflows (Breen et al. 2010b). The Forster & Caswell (1989) study revealed many instances where a number of maser sites are present in a small cluster on a scale of several hundred mpc, pinpointing individual high-mass constituents within an extensive star formation region (SFR).

The masers are valuable as a probe for discovering stars at the early stage when the star itself is not visible because of obscuration from the dust in the surrounding molecular cloud, and also

★E-mail: james.caswell@csiro.au

for measuring the physical parameters of the environment where the massive star is forming (Cragg, Sobolev & Godfrey 2002). Massive YSOs are found to host the three principal maser species in various combinations, prompting speculation that these combinations are clues to the evolutionary stage of the massive YSO (e.g. Breen et al. 2010a). For example, water maser emission at 22 GHz has sometimes been thought to be most prolific at an early stage of stellar evolution but, in fact, clearly extends to accompany later stages when OH masers and ultracompact H II regions are present. The reality is further complicated by some water masers found towards lower mass stars (Furuya et al. 2003). Finally, specific spots can be ephemeral, disappearing on a time-scale as short as months, to be replaced by generally similar emission in the same region but sometimes at a slightly different position and velocity.

Since the interplay between masers of different species is expected to be valuable in studying massive star formation, it is important that surveys for masers throughout sizable portions of the Galactic disc be conducted in an unbiased manner for each species. Large portions of the southern Galactic disc have been fully surveyed for 1665-MHz OH (Caswell 1998), and an even more extensive survey for 6668-MHz methanol masers is now producing its first results (Caswell et al. 2010). A large compilation of precise methanol positions is now available (Caswell 2009) based on small regions surveyed so far (Caswell 1996; Ellingsen et al. 1996), and supplemented by targeted searches (e.g. Caswell et al. 1995). In contrast, unbiased water maser surveys for sizable portions of our Galaxy have not been attempted to date. The problem is that large, sufficiently sensitive, telescopes at the high frequency of 22 GHz have small beams which make such surveys dauntingly time consuming.

Earlier water maser searches have chiefly been made at sites where the occurrence of other maser species is already known e.g. the extensive searches with the Parkes radio telescope towards southern star-forming regions, specifically OH maser sites, as reported by Caswell et al. (1989). However, the serendipitous discovery of isolated water masers demonstrates that such searches may reveal only the tip of the iceberg. An early unbiased survey was attempted 20 yr ago (Matthews et al. 1985); 2 $\deg^2$ were surveyed, with sensitivity varying between 2 and 7 Jy, and yielded 26 sources. It highlighted the desirability of a more homogeneous survey, of greater sensitivity. Another lesson learnt from that survey is the need to obtain accurate (arcsec) positions from the survey itself, or very shortly thereafter (to overcome some serious problems of variability). More recently (and observed subsequent to the present survey), a blind survey of a small (0.25-$\deg^2$) region was conducted by Breen et al. (2007), and a much larger single dish survey has begun (Walsh et al. 2008).

Here we describe an alternative attack on this problem, using the Australia Telescope Compact Array (ATCA) for the survey itself, and thus providing precise positions directly from the discovery observations. This pilot survey demonstrates a feasible strategy and provides significant first results. The ATCA mosaic observing mode is well suited to fast mapping, and allows efficient surveying for water masers at this high frequency where the primary beamwidth to halfpower is only 2.29 arcmin. For a survey strategy to be useful, sky coverage must be fast, but sensitivity need only be modest, since many masers are present with peaks that exceed 1 Jy.

Although the present exploratory study is confined to a quite small region, discovery statistics from even a small portion of blindly surveyed sky will provide a better guide to expectations from a full survey than any previous studies.

2 OBSERVATIONS AND DATA REDUCTION

The survey observations were made with the ATCA in the H168 array configuration over two sessions, 2004 July 30 and 2005 May 24 (project c1189).

Intensity calibration for both sessions is based on a flux density for 1934−638 of 0.98 Jy. Phase (position) calibration and bandpass calibration were based on regular observations of 1414−59 (1.43 Jy in the first session and 1.18 Jy in the second session) supplemented for bandpass calibration in the first session by the strong source 1921−293 (15.58 Jy).

The correlator sampled two orthogonal linear polarizations, processed to give a 256-channel spectrum across a 32-MHz bandwidth. The observing strategy in the first session was to observe a mosaic tile of 36 target positions (almost 30 s at each position), and then a calibrator. This was continued for eight adjacent mosaic tiles. The whole loop of eight mosaic tiles was then repeated so as to increase the *uv*-coverage and sensitivity. For the second session, a modified strategy used integration times of 20 rather than 30 s, so as to allow three loops rather than two loops, and used five tiles, each composed of 54 pointings. The mosaic pattern of the observed points was a triangular grid with minimum spacing of 144 arcsec = 2.4 arcmin ($0\overset{\circ}{.}04$) i.e. staggered rows spaced approximately 2 arcmin. The primary beam of the 22-m ATCA antennas at 22 235 MHz has a width to halfpower of 137 arcsec (2.29 arcmin). The furthest interior point from a grid sample is 83 arcsec (equidistant from three grid points, where the sensitivity is 0.34 times that at the beam centre). With this surveying strategy, 1 $\deg^2$ requires 625 (25 × 25) pointings, corresponding to 625 min, nearly 10.5 h. The total observing time for each session, including overheads, was nearly 6 h.

The first session covered a rectangular region of the Galactic plane bounded by longitudes $305\overset{\circ}{.}0$ and $306\overset{\circ}{.}26$, and latitudes $\pm0\overset{\circ}{.}15$ (288 points covering 0.46 $\deg^2$). The major and minor axes of the synthesized beamwidth to halfpower using the H168 array were 12.2 and 10.7 arcsec (major axis aligned approximately in right ascension). The second session covered a slightly smaller region (270 points covering 0.43 $\deg^2$) bounded by longitudes $311\overset{\circ}{.}0$ and $312\overset{\circ}{.}18$, and (again) latitudes $\pm0\overset{\circ}{.}15$. The beamwidth major and minor axes were 13.3 arcsec and 9.9 arcsec (the hour angle coverage was somewhat different from the first session).

The AIPS reduction package was used for data processing, following the general procedure described by Caswell (1997); in the realignment of channels using the CVEL program, the adopted rest frequency was 22 235.08 MHz, and the velocity scale was with respect to the local standard of rest (LSR). The corresponding centre velocities were −22 and −5 km s^{-1} in the first and second sessions, respectively. The channel separation was 1.68 km s^{-1}, and with uniform weighting of the correlation function the final velocity resolution was 2.0 km s^{-1}. With ATCA correlator constraints at that time, this relatively coarse resolution was the highest possible without sacrificing wide velocity coverage and recording of two polarizations. We discarded the extreme channels and retained 225 channels covering more than 28 MHz. This corresponds to a velocity coverage of 380 km s^{-1}, wide enough to recognize the possible presence of any high-velocity features representing outflows, for which the water masers are renowned.

Total intensity maps were produced of the channels with maser emission after subtraction of any underlying continuum. The rms noise on an individual channel map was typically 0.15–0.17 Jy.

A third (follow-up) session, 2007 October 9 (project c1762), was used to re-observe just the previously detected sources, primarily to obtain spectra of better spectral resolution and higher sensitivity, but also allowing an assessment of variability. The ultracompact H75 array (synthesized beamwidth approximately 25 arcsec) was used, and a correlator configuration recording a single linear polarization with 512 channels across 32 MHz was adopted. As noted by Caswell & Phillips (2008), typical water maser features are mostly less than 20 per cent polarized and we have treated the single polarization data as an acceptable approximation to total intensity. The loss of sensitivity incurred by sampling a single polarization was compensated for by observing with at least three cuts, each of 2 min or more, and varied according to expected source strength; in all cases this provided sensitivity at least twice as good as in the original survey. The position calibrator was 1352−63. The processing procedure was similar to that of the first two sessions. Improved spectra for the original survey sources were obtained, with independent position estimates adequate to assess whether the source at this second epoch coincided with the original survey source. Data were also inspected for any new sources that might have been absent from the initial surveys due to variability or lower sensitivity.

3 RESULTS

Table 1 is a complete list of the 32 maser sites detected. Two of them were detected only in 2003 or 2004 and six were detected only in the more sensitive observations of 2007. 17 were detected in 2003 and 2007, and seven were detected in both 2004 and 2007. Following the usual practice, the Galactic longitude and latitude of each source, listed in the first column, is used as an identifying source name for each water maser. For four sources previously measured by Breen et al. (2010b; hereafter BCEP) we use their designations, and in the 28 other cases with no previous detection the Galactic name is derived from our equatorial coordinates (J2000) given in Columns 2 and 3 (listed with greater precision than our Galactic coordinates). Positions listed from our measurements are from the initial survey observations wherever possible, since these were taken with the H168 array and thus have better spatial resolution than the follow up (H75 array) observations. Consistency with our later epoch observations suggests their rms uncertainty is 2 arcsec. Comparison with BCEP for four sources in common supports this conclusion and suggests that the BCEP position uncertainties (based on two independent measurements) are smaller than 2 arcsec, at least in this region of sky. The velocity range of emission is given in columns 4 and 5 (lowest and highest velocities), and is taken as the largest range seen at either of the observed epochs. The velocity of strongest emission and its peak intensity is then given, first for 2007 (identified as F = follow-up) and then for 2003 or 2004, the survey epoch (identified as S = 'survey'). Column 10 gives an estimate of the systemic velocity for each site, in most cases taken from the approximate velocity of strongest water maser emission,

Table 1. Water maser properties. 'Remark' abbreviations: BCEP – Breen et al. (2010b); bs(rs) – with blue(red)shift high-velocity feature.

Source Name	Equatorial Coordinates		Vel. range		Follow-up		Survey data		V_{sys}	Remarks
(l, b)	RA(2000)	Dec.(2000)	V_L	V_H	V_{pk}(F)	S_{pk}(F)	V_{pk}(S)	S_{pk}(S)		
(° °)	(h m s)	(° ′ ″)	(km s^{-1})		(km s^{-1})	(Jy)	(km s^{-1})	(Jy)		
305.120−0.087	13 10 39.37	−62 52 39.6	−41	−17	−35	1.2	−33	3.1	−30	
305.136+0.071	13 10 41.25	−62 43 05.9	+51	+53		<0.2	+52	1.3	+50	
305.138+0.067	13 10 42.66	−62 43 19.5	−42	−36	−38	1.6			−40	
305.191−0.006	13 11 13.58	−62 47 25.5	−60	+40	+33	23	+32	6.1	+30	BCEP; bs
305.198+0.007	13 11 16.91	−62 46 36.1	−42	−24	−40	7	−34	4.2	−35	BCEP
305.208+0.207	13 11 13.74	−62 34 40.6	−45	−34	−35	135	−38	70	−40	BCEP
305.269−0.003	13 11 53.82	−62 46 55.6	−83	−53	−60	0.8			−60	
305.271−0.007	13 11 54.94	−62 47 10.7	−40	−24	−35	3.3	−33	8.2	−35	
305.284−0.084	13 12 05.05	−62 51 41.6	−20	−11	−16	1.2	−17	0.9	−15	
305.322+0.070	13 12 18.35	−62 42 17.1	−96	−11	−30	258	−32	160	−35	bs, rs
305.361+0.150	13 12 35.82	−62 37 19.2	−45	−31	−35	313	−36	105	−35	BCEP
305.475−0.096	13 13 45.70	−62 51 27.8	−91	−50	−85	3.3	−83	0.7	−45	strong bs
305.553−0.012	13 14 22.78	−62 45 59.8	−45	−30	−35	4.5			−35	
305.561+0.013	13 14 25.68	−62 44 30.0	−48	−38	−42	0.7	−41	4.9	−40	
305.564+0.012	13 14 27.29	−62 44 30.9	−36	−34	−35	1.1			−35	
305.666−0.107	13 15 26.38	−62 51 02.8	−77	−59	−69	6.5	−63	0.9	−65	
305.726+0.082	13 15 48.50	−62 39 25.4	−55	−32	−44	6.2	−44	5.3	−45	
305.817−0.110	13 16 45.52	−62 50 22.2	−105	−40	−55	1.3	−51	4.3	−55	bs
305.822−0.115	13 16 48.55	−62 50 39.0	−45	−36	−38	4.8	−36?		−40	
305.834−0.082	13 16 52.94	−62 48 37.2	−125	+29	−113	23	−110	10.5	−45	dominant bs; rs
305.887+0.017	13 17 15.67	−62 42 23.3	−107	−24	−29	27	−28	22.5	−35	bs
305.943+0.029	13 17 44.12	−62 41 21.4	−49	−27	−41	4.8	−41	2.7	−40	
306.056−0.042	13 18 46.95	−62 44 52.2	−35	−20	−34	0.37	−28	3.5	−30	
311.230−0.032	14 02 27.48	−61 45 14.3	+15	+40	+29	20	+28.5	59	+30	
311.663−0.106	14 06 09.07	−61 42 17.8	−66	−30	−65	0.26	−36	0.8	−50	
311.811−0.087	14 07 17.62	−61 38 38.8	−60	−37	−58	0.2	−55	1.8	−50	
311.828+0.130	14 06 54.49	−61 25 52.0	−117	−5	−109	1.6	−114	1.2	(−50)	dominant bs; rs
311.838+0.129	14 06 59.36	−61 25 47.7	−49	−45	−48	1.2			−50	
312.013−0.035	14 08 47.73	−61 32 08.6	+16	+21		<0.1	+17	0.9	+20	
312.071+0.082	14 08 58.33	−61 24 24.2	−65	−15	−32	27	−32	23.2	−35	bs
312.094+0.074	14 09 10.09	−61 24 24.9	−92	−39	−49	7.5	−40	2.1	−45	bs
312.114+0.009	14 09 29.32	−61 27 49.7	−55	−27	−42	9.8	−47	8.8	−45	

but in a few cases modified by consideration of other information discussed for each source in Section 4. Column 11 includes miscellaneous notes on some sources, noting the previous water detection for four sources and drawing attention to high-velocity outflows.

The spectra of 30 masers shown in Fig. 1 are all taken from the 2007 follow-up observations over a single 8-h period. Spectra are effectively time-averaged over several cuts spread over the session. Any sidelobe of a strong source can be readily identified since the spectrum showing the sidelobe has been obtained from observations interleaved with those of the strong on-source measurement and thus retains its spectral signature, unaffected by possible time variability. Two masers detected only in 2003 or 2004 are not shown since they have simple spectra adequately characterized by the peak intensity, its centre velocity and range, given in Table 1.

The spectrum of 305.322+0.070 shows it to be the strongest new source. 305.475−0.096 was the weakest in the initial survey observations (peak of 0.7 Jy after applying a primary beam correction to the raw value of 0.4 Jy observed at an offset from the pointing centre); 305.284−0.084 and 305.666−0.107 were also below 1 Jy. Most sources are quite distinct from others nearby, with no confusion in the spectra. Exceptions are discussed in Section 4.

4 INDIVIDUAL SOURCES

The following notes contain details for individual sources that are not adequately conveyed in the table or from the single epoch spectra shown.

305.120−0.087. A new maser site with a reliable detection at two epochs, but weaker at the second epoch by a factor of 3.

305.136+0.071. This new maser was detected only at the first epoch, fading by a factor of at least 6 by the second epoch observation three years later. It is a single feature, adequately characterized by its intensity, velocity and width given in Table 1, and no spectrum is displayed. Its positive velocity indicates a distant location outside the solar circle.

305.138+0.067. New maser detected only at the second epoch in the field targeting the previous maser. It is a single feature at a negative velocity, quite different from the previous source, and in the most common velocity range for this region of sky. It is spatially offset from the previous site by 17 arcsec and thus quite distinct and unlikely to be related, especially in view of its quite different velocity.

305.191−0.006. This source, unreported at the time of the survey, was independently detected as a new source by BCEP while searching towards a nearby OH maser at a quite different velocity. The velocity of its main feature is persistently (at four epochs over a 4-yr time-span) at $+32$ km s^{-1}, but with intensity varying by a factor of at least 4. The positive velocity indicates a distant location outside the solar circle. Within a few arcsec, our 2007 measurements show features weaker than the main emission by a factor of more than 5, near -40 km s^{-1}. We interpret these features as part of the same maser site, representing high-velocity emission, blueshifted by more than 70 km s^{-1} from the main feature. They were not detectable in our initial survey observations of 2004, nor in the BCEP observations in 2003 and 2004. Note that the nearby source 305.198+0.007 also has features near -40 km s^{-1}, but Fig. 1 reveals that the spectral details are quite different, and the position is offset by 54 arcsec.

305.198+0.007. This source was independently discovered in observations by BCEP. The overall velocity range has remained similar over four epochs, with variations in peak intensity by a factor of 2. There is no methanol maser coincident with the water maser site 305.198+0.007, but the methanol site 305.199+0.005 (Caswell 2009) is offset by slightly more than 10 arcsec. This separation of the water and methanol sites is sufficiently large to rule out the same source of excitation, but close enough in projection, and with similar velocity, to indicate that they are separate star-forming sites within the same stellar cluster, with systemic velocity best defined by the methanol maser (see Section 5.4.3).

The negative feature at $+32$ km s^{-1} in our spectrum of 305.198+0.007 is merely a weak sidelobe response to the strongest feature of the unrelated water maser site 305.191−0.006 which is 54 arcsec away (see previous note).

305.208+0.207. This is a strong source which lies outside the boundary of our intended survey region but was clearly detected during the survey processing despite the large offset (248 arcsec) from the nearest pointing centre. The survey observation required a large primary beam correction factor which is uncertain to within a factor of 2, but the follow-up observation of 2007 was centred on the source position. The source was also detected as a strong maser (peak exceeding 200 Jy) by BCEP, with emission confined to the same small velocity range seen in our data, and similar to that of its associated OH and methanol emission. It almost certainly corresponds to the strong water maser reported at approximately this position in the early (epoch 1976) single dish Parkes observations by Batchelor et al. (1980).

305.269−0.003 and 305.271−0.007. The second site appeared similar in both the discovery survey and its follow-up, although weaker by a factor of 2 at the second epoch. However, the first source, 305.269−0.003, is weak and detected only in the 2007 follow-up observations to its companion and offset 17 arcsec from it. In our spectrum of 305.269−0.003, a sidelobe response to the companion, 305.271−0.007, is evident.

305.284−0.084. This new maser has a simple spectrum with narrowly confined velocity range, showing very little change between our two observing epochs.

305.322+0.070. Of our new, previously unreported, discoveries, this maser is the strongest. It displays prominent emission in the velocity range -50 to -30 km s^{-1} exceeding 200 Jy, generally similar at both epochs. Weak high-velocity emission is present extending to a highly blueshifted velocity of -95 km s^{-1}, and to a redshifted velocity of -11 km s^{-1}.

305.361+0.150. This strong maser was also reported by BCEP, with peak emission exceeding 100 Jy, and limited to the same small velocity range seen in our data, similar to that of its associated OH and methanol emission. It almost certainly corresponds to the strong water maser reported at approximately this position in the early (epoch 1977) single dish Parkes observations by Batchelor et al. (1980).

305.475−0.096. A similar velocity range of emission was detected at both epochs. Features at both velocity extremes were of similar intensity at the first epoch, and the systemic velocity is likely to be near -45 km s^{-1}. The intensity of the blueshifted high-velocity feature increased by more than a factor of 4 at the second epoch.

305.553−0.012. This source was detected only at the second epoch, offset from the field centre used to target masers 305.561+0.013 and 305.564+0.012.

305.561+0.013 and 305.564+0.012. These two masers are separated by only 11 arcsec. Their spectra displayed in Fig. 1 are aligned in velocity, and it is clear which single feature arises from which source. 305.561+0.013 was five times stronger in the survey data than at the follow-up epoch. In contrast, 305.564+0.012 was

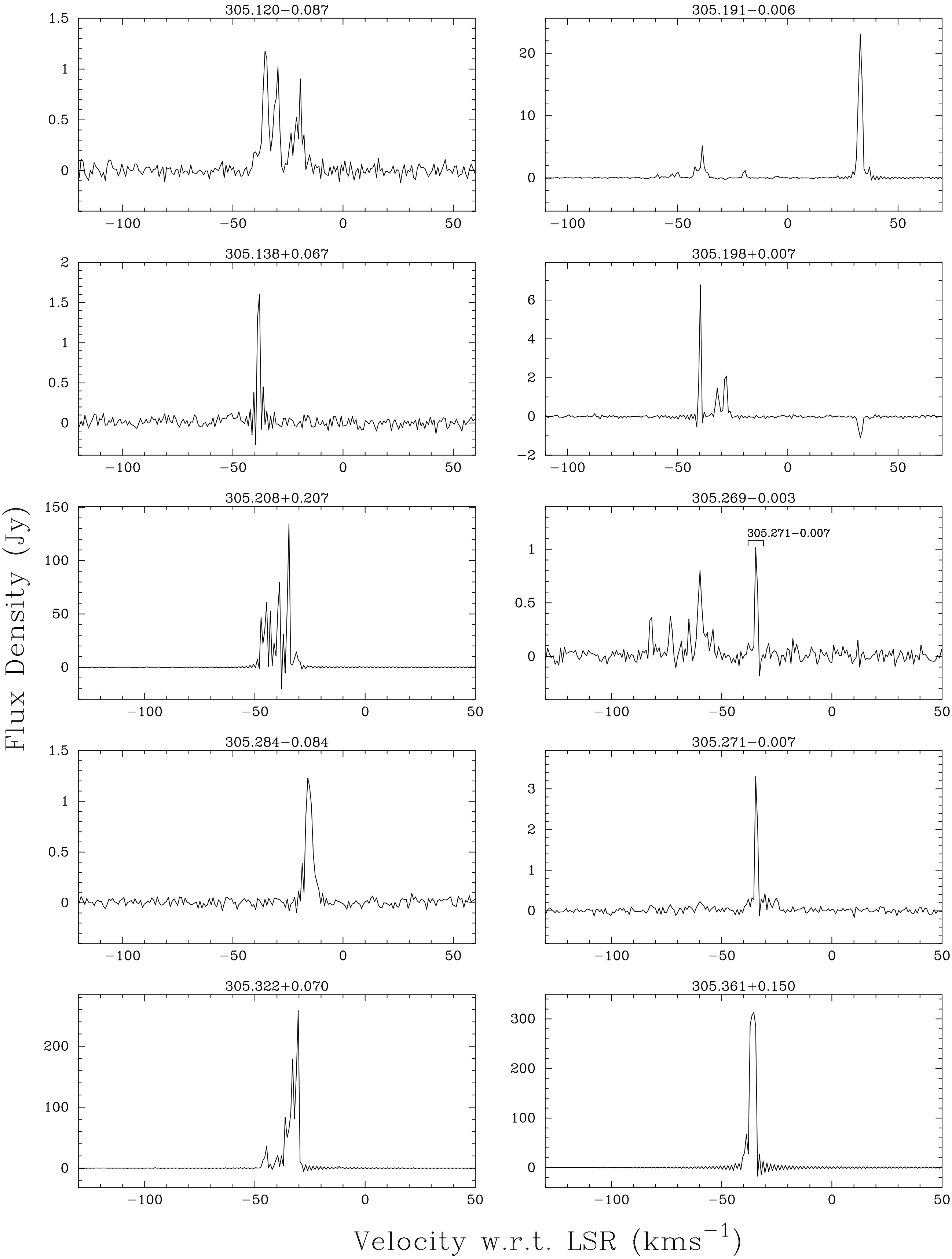

Figure 1. Spectra of 22-GHz water masers detected in pilot survey.

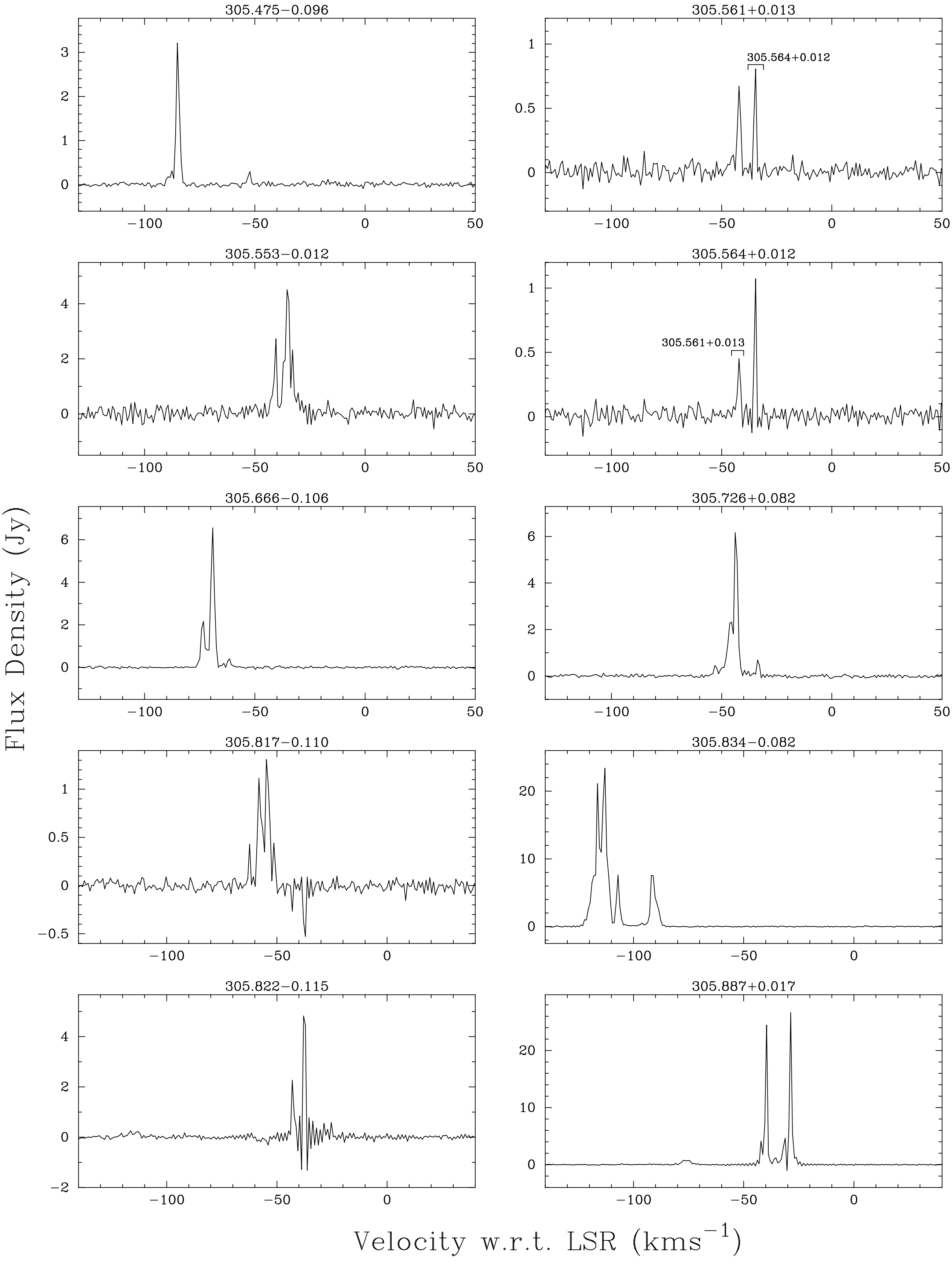

Figure 1 – *continued*

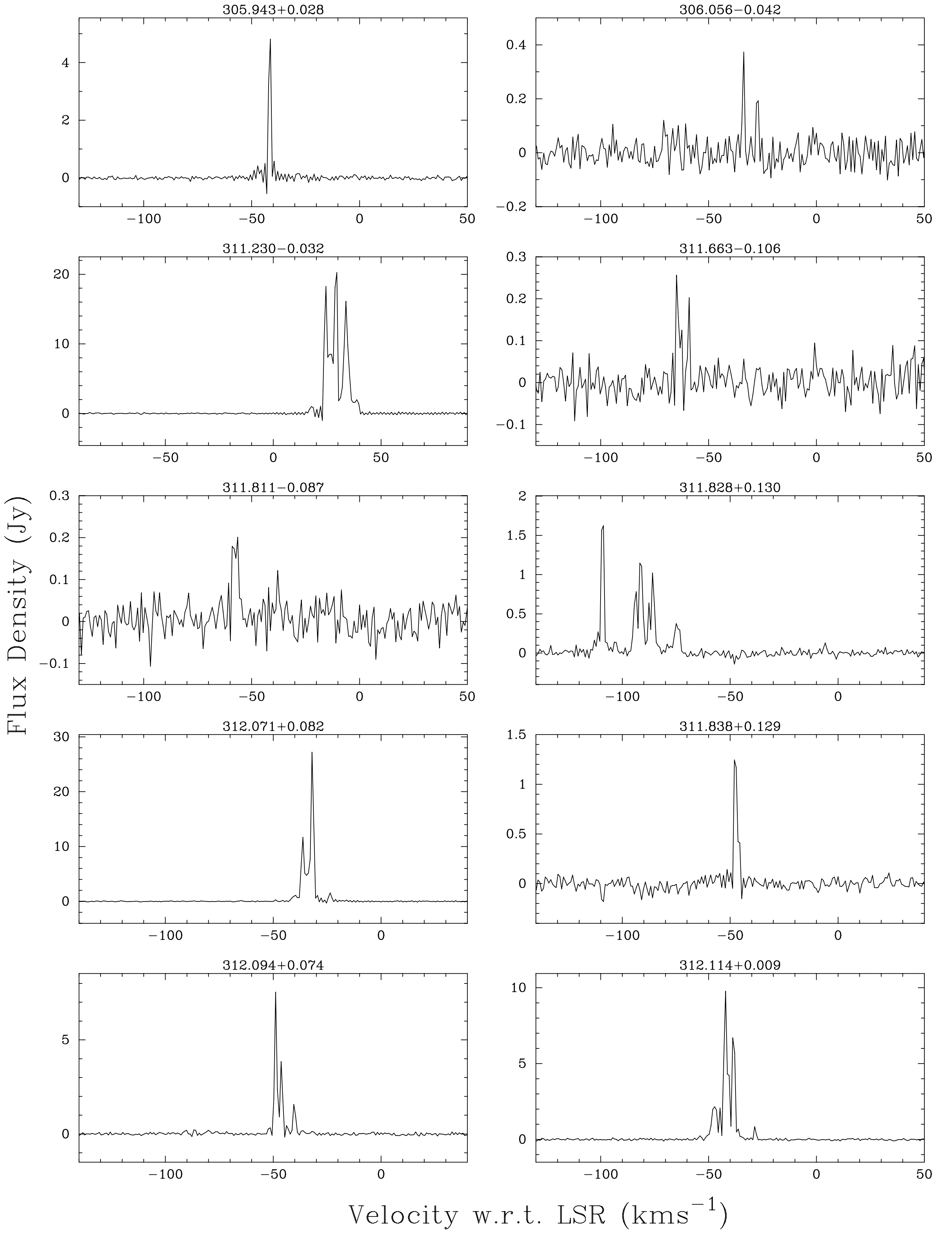

Figure 1 – *continued*

detected only at the follow-up epoch, as a chance discovery while targeting 305.561+0.013.

305.666−0.107. This source was a weak single feature at the discovery epoch and increased by the follow-up epoch to show many more features, two of them stronger than the original.

305.726+0.082. No major changes between the two observing epochs occurred at this site.

305.817−0.110 and 305.822−0.115. The separation of these two masers is 29 arcsec, and we have aligned their spectra so as to clearly reveal the weak negative sidelobe response to each source at the position of the other. 305.817−0.110 was detected at both epochs, with peak intensity weaker at the follow-up epoch by a factor of 3. At the survey epoch, it clearly showed a high-velocity blueshifted peak of 1.3 Jy at -105 km s^{-1}. 305.82−0.115 was detected only at the follow-up epoch. The weak apparent emission seen between -105 and -110 km s^{-1} is a weak sidelobe response to the strong maser 305.834−0.082 (see notes for next source).

305.834−0.082. The strong features between -105 and -120 km s^{-1} increased from a peak of 10.5 Jy at the survey epoch to 23 Jy at the follow-up epoch. At the survey epoch, weak features extended to $+29$ km s^{-1}, including one at $+25$ km s^{-1} with a peak of 0.7 Jy. Near Galactic longitude 305°, the systemic velocity is unlikely to be near -100 km s^{-1}, and most likely lies between -55 and -35 km s^{-1}, indicating that the emission is dominated by a blueshifted outflow. With this interpretation, there is a weak accompanying redshifted outflow, but negligible emission near the systemic velocity itself. These properties are characteristic of the class of water maser dominated by blueshifted outflows recognized by Caswell & Phillips (2008).

305.887+0.017. This is a strong maser showing little change between survey and follow-up epochs. It coincides with a methanol maser (Caswell 2009), and the velocities of strongest water maser emission are similar to the methanol velocity near -35 km s^{-1}, which we adopt as the systemic velocity. Weak emission extending to -107 km s^{-1} thus corresponds to a blueshifted outflow.

305.943+0.029. Emission at both epochs is similar, although slightly stronger at the follow-up epoch.

306.056−0.042. This maser showed quite strong emission at the survey discovery epoch and faded at the follow-up epoch by an order of magnitude.

311.230−0.032. The many strong features of this maser are all at positive velocity in the range $+15$ to $+40$ km s^{-1}, almost certainly characteristic of the systemic velocity and indicating a distant location outside the solar circle.

311.663−0.106. This maser is quite weak on the follow-up spectrum, only one-third the intensity of the discovery spectrum.

311.811−0.087. This is the weakest of our confident detections at the follow-up epoch. The two features were an order of magnitude stronger at the discovery epoch when it was a readily detectable source.

311.828+0.130. At both epochs, strongest emission is at a large negative velocity near -110 km s^{-1}. The spectrum (Fig. 1) from the follow-up observations clearly shows weaker emission extending to -73 km s^{-1}. A small negative feature near -48 km s^{-1} is a weak sidelobe response to 311.838+0.129 (see note for next source). The weak feature of 0.13 Jy at -5.9 km s^{-1} is close to the noise threshold but just significant. With a total velocity range from -117 to -5 km s^{-1} it seems most likely that the site has a systemic velocity near -50 km s^{-1} (as for the nearby source 311.838+0.129) where there is no detectable emission, and the main features are from the high-velocity blueshifted outflow. The feature at -6 km s^{-1} arises from a weak outflow, redshifted relative to the systemic velocity.

311.838+0.129. This maser was detected only in the follow-up observations, while targeting 311.828+0.130 (offset by 35 arcsec) and is confined to a small velocity range near -50 km s^{-1}. The weak negative signal at high negative velocities is a sidelobe response to 311.828+0.130, as is clear from the alignment of their spectra in Fig. 1.

312.013−0.035. This maser was clearly detected in the initial survey observations but had faded by more than a factor of 5, to become undetectable at the detection threshold of the follow-up observations. Its simple spectrum is not shown since it is adequately characterized by the parameters of Table 1. The positive velocity probably indicates a distant location outside the solar circle.

312.071+0.082. This new maser showed strong emission between -40 and -30 km s^{-1} at both epochs. A weak feature of 0.17 Jy at -65 km s^{-1} is a high-velocity blueshifted feature.

312.094+0.074. A cluster of features at both epochs is prominent between -50 and -40 km s^{-1}, and thus assumed to span the likely systemic velocity. A 2-Jy feature was present at -72 km s^{-1} in the survey epoch spectrum, and weaker, but more highly blueshifted, features are present in the follow-up spectrum (Fig. 1) near -90 km s^{-1}.

312.113+0.009. Strong emission is present at both epochs, confined to the modest velocity range -55 to -27 km s^{-1}, which most likely encompasses the systemic velocity.

5 DISCUSSION

5.1 Detection statistics and variability

Our rms noise in the initial surveys was typically 0.15 Jy, allowing us to recognize sources as weak as 0.4 Jy in favourable circumstances of lying near a pointing centre and if the velocity width covered several channels. Our source list is conservative and limited to confident detections since the insidious effects of spurious sources are far greater than the failure to note a marginal detection. Our sparse pointing coverage did not provide uniform sensitivity within the outer boundary of our survey regions; the sensitivity varies by a factor of nearly 3 between a location coincident with a telescope pointing and a location equidistant from the three nearest pointings. Some of this loss of sensitivity can be recovered by combining three adjacent pointings, after which the worst sensitivity is 0.59 relative to a pointing centre. Factors correcting peak intensities for their offset from the pointing centre were applied to all sources and ranged from 1.02 to 2.5 (plus a factor of 50 for one source that was very strong and lay outside the intended boundary of our search area).

Combining the statistics from measurements at the survey epochs and the follow-up epoch, we detected a total of 32 distinct water maser sites in an area of 0.89 deg^2. Only four of these water maser sites clearly correspond to masers previously reported (BCEP), originally discovered during targeted observations towards a few methanol and OH masers in the region. All 32 masers had a peak flux density of at least 0.8 Jy in at least one of two observing epochs, and 29 had a peak flux density exceeding 1 Jy in at least one observing epoch. Only 17 exceeded 1 Jy at two observing epochs. The smallest separation between neighbouring sources was 11 arcsec, for 305.561+0.013 and 305.564+0.012, a separation most likely indicating excitation by different hosts within the same star-forming cluster.

23 masers were detected in the first region, of area 0.46 deg^2, the weakest maser having a peak flux density of 0.8 Jy, and nine were detected in the second region, of area 0.43 deg^2, the weakest with

a peak of 0.84 Jy. The regions chosen for this exploratory survey deliberately avoided the previously known parts of the Galaxy most densely populated with massive star formation tracers such as H II regions, methanol masers and OH masers. In the first region near longitude 305°, where there was existing evidence of only modest star formation, we find that the water maser space density surpasses that of methanol or OH masers in even the portion of Galactic disc where they are known to be most profuse [e.g. near Galactic longitude 330° (Caswell 1996) or near the Galactic Centre (Caswell et al. 2010)]. Our second pilot region near longitude 311° had no previously reported massive star tracers and yet showed a quite high density of water masers.

From the relatively small region covered by this pilot study, we cannot reliably assess a typical space density of sources in the Galaxy, but we have established a lower limit in the area of interest which is surprisingly high. It is clear that extensive surveys to sensitivity limits slightly below 1 Jy will be enormously productive.

Masers of methanol and OH commonly display several spectral features, most of them undergoing only minor changes over time-spans of several years, so that the spectrum can be used as a unique identifying 'fingerprint' for each source. In contrast, the unique identity of a water maser is not well characterized by its spectrum. Extreme variability over less than two years often occurs, and successive spectra are not recognizably from the same site. However the position, measured to arcsecond accuracy, does remain stable, and is the only reliable identifier for each water maser site (BCEP).

The variability monitoring of 43 water maser sites over 20 yr by Felli et al. (2007) is an excellent demonstration of the enormous fluctuations that occur on many time-scales. These provide strong evidence that over several decades, although individual maser spots at a site may come and go, the activity from each site is persistent on long time-scales, compatible with the common belief that the sites may have water maser lifetimes as long as 10^4 yr. In accord with expectations from the Felli et al. study and the BCEP observations, we find marked variability between the two epochs of our observations. Our follow-up observations had better spectral resolution than the initial survey, and narrow features are therefore expected, on average, to have larger peak intensities than at the survey resolution; in line with this expectation, the median of the distribution of peak flux densities increases from 2.9 Jy in the survey to 4.0 Jy in the follow-up. However, this bias cannot be responsible for most of the variability observed since there are masers showing reduced intensity in the follow-up observations, and there are relative intensity changes between features within a spectrum.

We found 26 sources in our initial survey observations, of which two had faded below detectability several years later in the follow-up observations. In fact, a further three follow-up detections were below 0.4 Jy and thus a total of five sources would have been undetectable if the follow-up observations had been restricted to the same sensitivity as the initial survey. Six sources were detected in the follow-up observations but had not been recognized in the survey observations. These small number statistics are compatible with variability expectations from the BCEP data for several hundred masers. Five or six sources from a total of 26 detected at one epoch but not at the second epoch are significant but not large. The statistics could be used to give a preliminary estimate of 'correction factors' needed if we make a survey at a single epoch but wish to determine the size of the underlying total population, i.e. including those sources that are temporarily dormant or quiescent at the time of the survey.

If we had relied on similarity of the spectra (rather than precise positions) for comparing the data at the two epochs, we would have interpreted the second epoch data as detecting only approximately half of the original detections, accompanied by the discovery of a similar number of new sources. This clearly has a large impact on guiding future surveys and emphasizes the great value of ascertaining precise positions at the initial survey epoch.

5.2 Evaluation of the survey strategy

Overall, the survey strategy appears to be an effective means of conducting a large-scale search for water masers in the Galactic disc. Employing integrations corresponding to three cuts each of 20 s, and the H168 array configuration of the ATCA, appears most appropriate. An alternative strategy is being pursued in the HOPS project (Walsh et al. 2008) to conduct a water maser survey which makes excellent use of the single 22-m dish Mopra antenna in the summer season when other demands for this telescope are low. The HOPS project is intended to cover the Galactic disc extending to latitudes $\pm0\overset{\circ}{.}5$ over the longitude range 300° through the Galactic Centre to 30° in a mode that provides coverage in 8 h of 1 $\deg^2$ (and hence 1° of longitude for this latitude coverage). Follow-up time on the ATCA is then needed to determine precise positions. For comparison, the ATCA survey that we have tested would take 12 h to cover 1 $\deg^2$, and achieves slightly better overall sensitivity (and significantly better sensitivity in an uneven pattern near the mosaic pointing centres); it uses a facility subject to greater demand than Mopra in the summer season, but precise positions are obtained in the ATCA survey itself, which then requires no follow-up. If both surveys are conducted, they could complement each other very well. For example, if the ATCA survey trialled here were to be limited to the narrow latitude coverage where the space density of masers is highest and most in need of high spatial resolution to avoid confusion, then the HOPS results would provide useful coverage to higher latitudes. A further planned complement with the ATCA is to conduct targeted measurements towards all of the approximately 1000 methanol masers from the methanol multibeam (MMB) survey (Green et al. 2009; Caswell et al. 2010). We note that the imminent completion of a new correlator on the ATCA will greatly increase the survey value, providing higher spectral resolution simultaneous with recording all polarization information, and a wide bandwidth channel with good continuum sensitivity. Spare correlator capacity will allow simultaneous coverage of other spectral lines such as ammonia and methanol.

5.3 Relationship of water to methanol and OH masers

Two water masers, 305.208+0.207 and 305.361+0.150, coincide with previously reported sites of methanol with OH maser emission, as noted by BCEP; indeed, these strong water masers are probably the same as those first noted by Batchelor et al. (1980), although the precise positions were not known until the BCEP measurements. The only other reported maser coinciding with one of our water masers is a methanol counterpart (Caswell 2009) to 305.887+0.017. There is no water maser at two other reported methanol maser sites in the surveyed region (Caswell 2009). However, the MMB survey (Caswell et al. 2010) has obtained new, preliminary, unpublished results for these regions, showing a further seven methanol sites, of which five have associated water masers. We thus have totals in these regions of 32 water masers and 12 methanol masers, of which eight sites are in common. The number of water masers at these survey sensitivities is thus 2.6 times greater than the number of methanol masers. Extension of the water maser surveys to larger areas is needed to refine this statistic.

5.4 Understanding the water maser velocities

It is well known that the velocity range of water masers is commonly much larger than that of methanol or OH masers, a fact clearly demonstrated in comparisons made by BCEP for several hundred water maser sites which have methanol and OH associations. Consequently, it is often difficult to estimate the systemic velocity of a water maser, and it is then difficult to assess whether velocity extremes are due primarily to a blueshifted or a redshifted component (or both). In order to understand the velocity information from the water masers in the present survey, we first assess methods of estimating their systemic velocities and then review comparison data from BCEP before considering the detailed velocity properties of the present sample.

5.4.1 Velocities of other SFR tracers in this region of Galaxy

Commonly used tracers of massive SFRs include H II regions, methanol masers and OH masers. These tracers generally have velocities dominated by Galactic rotation, and meaningful kinematic distances can be estimated for them. Furthermore, sources are concentrated within spiral arms, especially those portions interior to the solar circle. Consequently, for any small Galactic longitude range, systemic velocities for these tracers are often limited to a few well-defined ranges.

For our pilot region centred near longitude 305°.6, nearby SFR tracers between 305°.0 and 306°.4 include 10 methanol masers (Caswell 2009), of which six also show OH maser emission. All have velocities between −43 and −24.4 km s^{-1}. Radio recombination lines of H II regions here show a similar range of velocities but, at longitudes only slightly outside the region, the H II regions 303.500−0.700, 303.115−0.947 and 302.504−0.749 show velocities of +32, +26 and +31 km s^{-1} (Caswell & Haynes 1987). Thus, we may expect most of the water masers in this region to also have systemic velocities clustered around −30 km s^{-1}, with possibly some near +30 km s^{-1}.

For our pilot region centred near longitude 311°.6, nearby SFR tracers include 14 H II regions listed by Caswell & Haynes (1987) with radial velocities and three methanol masers listed by Caswell (2009). 11 H II regions and two methanol masers have negative velocities in the range −61 to −38 km s^{-1}, and three of the H II regions and one methanol maser have positive velocities, all of them in the range +32 to +36 km s^{-1}.

In both pilot regions, a velocity of −61 km s^{-1} approximately corresponds to the largest negative velocity possible at this longitude for material whose motion is dominated by Galactic rotation, and corresponds to a distance of about 5.3 kpc. The smaller negative values correspond to distances larger or smaller than this by several kpc (and a small value between 0 and −20 km s^{-1} may corresponds to local material within a few kpc). In contrast, the significant positive velocities indicate locations outside the solar circle, at a distance greater than 11 kpc, probably in the Carina arm.

5.4.2 Velocity properties of previously studied water masers

The velocity structures of sources from our new survey (to be discussed in the next subsection) were puzzling, and prompted us to revisit analogous results from earlier observations. No suitable analysis seems yet to have been reported, so we decided to use the large sample of water masers recently reported by BCEP and perform a new analysis on it. The sample has wide velocity coverage, sensitivity which is good and fairly uniform, and positional accuracy able to confirm that all listed velocity features lie close to a single position. BCEP note that water masers generally have a wider velocity range than OH and methanol masers, but the water maser peak emission is usually within 30 km s^{-1} of the systemic velocity (as estimated from velocities of associated methanol or OH maser emission). However, there are sometimes features extending outside this range which are commonly referred to as high-velocity features, and we are especially interested in these since there has been no previous study of the characteristics of such features from a large sample of water masers.

In order to investigate high-velocity features, we require an estimate of the systemic velocity of each source and a decision on what size offset to define as 'high velocity'. In the BCEP sample of water masers, there are 229 water masers with an associated methanol or OH maser; in these cases, we can use the velocity of peak methanol emission (or of OH in the 33 cases where there is no methanol) to characterize the systemic velocity. We note that the mid-range (rather than the peak) velocity of methanol or OH emission is probably a better estimate, but our simpler choice (using the data from table 3 of BCEP) has negligible effect on our results. We define high velocity as an offset from systemic of more than 30 km s^{-1}. We distinguish between sources showing features shifted only to the red, only to the blue and those showing both. We combine data from both epochs (179 observed in 2003, 191 in 2004 and thus some masers observed at both epochs), so classification of a high-velocity feature corresponds to the feature seen in either epoch or both.

With these criteria, the high-velocity features fall into three categories: 31 masers show only blueshifted features, 25 show both red and blue and 21 show only red. 152 masers show no high-velocity features. Thus there is a slight preponderance of blueshifted features. Note that the blueshifted sources include 351.273+0.641 and 291.270−0.719, two of the sources described as dominant blueshifted outflows by Caswell & Phillips (2008); however, another dominant blueshift outflow source, 351.243+0.671, is in the 'red+blue' category since it showed weak redshifted emission as well as dominant blueshifted emission during the BCEP measurements. We now distinguish between water masers associated with only methanol (70), those with both methanol and OH (126) and those with only OH (33). Since the sample sizes differ, comparisons are best expressed by the frequency of occurrence of high-velocity outflows of water maser emission as a percentage of the sample.

For water with only methanol associated, we find 31 per cent with outflows:

16 per cent blue (11 sites), 7 per cent 'blue+red' (5 sites) and 8 per cent red (6 sites).

For water associated with both methanol and OH, we find 34 per cent with outflows:

14 per cent blue (18 sites), 10 per cent 'blue+red' (13 sites) and 10 per cent red (12 sites).

For water associated with only OH, we find 39 per cent with outflows:

9 per cent blue (3 sites), 21 per cent 'blue+red' (7 sites) and 9 per cent red (3 sites).

These are small samples, but it is noticeable that as we move from methanol to 'methanol with OH' and finally to OH, the percentage of sources with high velocity of any type increases only slightly from 31 to 34 to 39. The percentage with redshift only is essentially unchanged (from 8 to 10 to 9). The percentage of blueshifts falls from 16 to 14 to 9, and is matched by an increase for 'red+blue' from 7 to 10 to 21.

Although the statistics do not justify strong conclusions, we note that if the sequence is treated as broadly representing evolutionary stages, then the final stage (OH without methanol) is consistent with the most common outflows being those where blue and red are both present; the small equal numbers showing red or blue are compatible with also being 'red+blue', but with red or blue randomly stronger and thus with their counterpart of opposite shift being slightly below detectability levels.

The earliest stage, of methanol only, suggests that the total fraction of masers which exhibit some variety of outflow is substantially the same as in the later stages, but a subset of these have the blueshifted emission unusually strong in the early stages. As they evolve, this subset progresses to showing both red and blue equally prominent.

Other statistics that might be considered could take into account the intensity, and simply categorize any source with both blue and red as predominantly blue or predominantly red, depending on which shift had stronger features or the larger number of features. However, we will not pursue such details here, since our primary purpose is to provide a yardstick against which to compare the new survey. Furthermore, the reality of this effect will soon be assessable from the follow-up of methanol masers from the MMB survey which will substantially increase the samples of water masers in the two categories associated with just methanol and 'methanol with OH'.

We finally note that the suspicion of an excess of blueshifts over redshifts was voiced in early studies when the sample of water masers was quite small (see e.g. Batchelor et al. 1980). However these earlier observations were hampered by the lack of instantaneous wide velocity coverage, and it was common practice after a high-velocity feature had been noticed at one epoch to take subsequent spectra centred between the high-velocity feature and systemic, to the exclusion of potential high-velocity features shifted in the other direction. So, confidence in the reality of the effect was low, and our new investigation suggests that the issue is more complex than a simple excess of blueshifts.

5.4.3 *Velocities of water masers in this survey*

In the first pilot region, three of the water masers coincide with a reported methanol maser, the preferred reliable means for assessing their systemic velocity. As noted in Section 4, another water maser, 305.198+0.007, apparently lies in a stellar cluster containing methanol maser 305.199+0.005, and most likely also the OH/methanol maser pair 305.200+0.019; these provide corroboration of the systemic velocity, -35 km s^{-1}, for this complex. For most of the remaining 19 masers, the velocity of peak water emission lies within the major velocity groupings recognized from other SFR tracers in the vicinity: the majority have velocities between -65 and -30 km s^{-1}; two have positive velocities and are likely to be distant objects beyond the solar circle and one has a velocity of -15 km s^{-1} and may be nearby.

In the second pilot region, none of the nine detected water masers coincides with a previously reported methanol or OH maser but, again, their velocities of peak water emission lie mostly in the two expected major velocity groupings: two have positive velocities and are likely to be distant objects beyond the solar circle; six have velocities between -50 and -35 km s^{-1} and are likely to lie within a few kpc of the tangent point.

Thus for our detected water masers which have no direct counterpart amongst other maser species or compact H II regions, the water velocities generally correspond to one of the two major velocity groupings of other SFR tracers in the vicinity of the survey regions and validates our use of these velocities in most cases as satisfactory estimates of systemic velocities, as listed in column 10 of Table 1.

Two remarkable exceptions are 305.834$-$0.082 with velocity near -110 km s^{-1} and 311.828+0.130, which has most of its emission near the remarkably high negative velocity of -114 km s^{-1}. These are 'forbidden' velocities according to Galactic rotation models and we interpret them to indicate blueshifted outflows from regions whose systemic velocities lie between -60 and -40 km s^{-1}. We regard them as likely members of the class of water masers dominated by blueshifted outflows. Caswell & Phillips (2008) list four members, and another excellent candidate, 320.255$-$0.305, was reported by BCEP. The fact that our unbiased survey of only a very small part of the Galaxy has increased the population from five to seven suggests that there may be quite large numbers which will only be discovered by such unbiased surveys. This would be consistent with the finding by Caswell & Phillips (2008) that none of their examples has an OH counterpart, three have only weak methanol counterparts and one has no other maser counterpart. Likewise, 320.255$-$0.305 has no other maser counterpart.

We now inspect the distribution of all extreme high-velocity features, irrespective of their intensity. If we regard an offset of 30 km s^{-1} from systemic as the threshold for the high-velocity definition, then nine (28 per cent of our sample) show high-velocity emission. Surprisingly however, of the 32 sites, there are none with redshifts, but six with just blueshifts and three with both blueshift and redshift; amongst the latter are 305.834+0.082 and 311.311.828+0.130, which are sources also exhibiting dominant blueshifted emission, much stronger than the redshifted outflow. If we strengthen the criterion to an offset of 50 km s^{-1}, then we reduce the number to a subset of five with blueshifts and one with both blueshift and redshift.

This excess of blueshifts is striking and we are not aware of any observational bias that would lead to this result since our velocity range extends much beyond 100 km s^{-1} from systemic towards both blueshift and redshift. However, we recall from the previous sub-subsection that an excess of blueshifts was also found in the BCEP sample selecting only water masers that had a methanol counterpart but no OH.

If the distribution of blue and red outflows were the same as that of the methanol-associated water sample from BCEP, this would forecast the presence amongst 30 masers of 4.7 with blueshifts, 2.1 with 'blue+red' and 2.6 with redshifts, a total of 9.4 high-velocity sources. Our survey sample of 30 water masers (where we have discarded the two water masers with an OH association – they do not show high-velocity emission) contains six with blueshifts and three with 'blue+red', i.e. similar to the 'forecast' for the total number of sources with high-velocity features and a similar preponderance of blueshifts. It is a much better match to expectations from the methanol-associated masers than to expectations from the OH-associated masers or 'methanol with OH'-associated water masers. This may be an indication that our unbiased survey has detected a large proportion of masers in the early evolution stage. Despite the small number statistics, we speculate that the population in our blind survey may even be dominated by an evolutionary phase preceding the methanol-associated sources, in which the bias to blueshifted outflows may be similar to, or even greater than, the bias shown by the methanol-associated water masers.

6 CONCLUSIONS

We have shown that our surveying mode is a practical strategy for extending unbiased water maser surveys to a large portion of the Galactic plane and results at two epochs show quantitatively the effect of variability on the completeness of single epoch surveys. We have demonstrated the high spatial density of water masers in typical portions of the Galactic disc, and our discovery of two new water masers dominated by high-velocity blueshifted outflows suggests that this class of object may be surprisingly common. We also find a striking preponderance of blueshifted high-velocity features relative to redshifted features, perhaps higher in this blind survey than in surveys targeting methanol or OH masers. This finding is compatible with dominant blueshifts being a characteristic of a population consisting chiefly of masers at the earliest evolutionary stage of star formation, in some cases prior to the onset of methanol masers.

ACKNOWLEDGMENTS

We thank Naomi McClure-Griffiths for generous advice and assistance in optimizing our mosaic mode of observing, and Simon Ellingsen for helpful comments that improved the manuscript.

REFERENCES

Batchelor R. A., Caswell J. L., Goss W. M., Haynes R. F., Knowles S. H., Wellington K. J., 1980, Australian J. Phys., 33, 139
Breen S. L. et al., 2007, MNRAS, 377, 491
Breen S. L., Ellingsen S. P., Caswell J. L., Lewis B. E., 2010a, MNRAS, 401, 221
Breen S. L., Caswell J. L., Ellingsen S. P., Phillips C. J., 2010b, MNRAS, doi:10.1111/j.1365-2966.2010.16791.x (BCEP)
Caswell J. L., 1996, MNRAS, 279, 79
Caswell J. L., 1997, MNRAS, 289, 203
Caswell J. L., 1998, MNRAS, 297, 215
Caswell J. L., 2007, in Chapman J. M., Baan W. A., eds, Proc. IAU Symp. 242, Astrophysical Masers and their Environments. Cambridge Univ. Press, Cambridge, p. 194
Caswell J. L., 2009, Publ. Astron. Soc. Australia, 26, 454
Caswell J. L., Haynes R. F., 1987, A&A, 171, 261
Caswell J. L., Phillips C. J., 2008, MNRAS, 386, 1521
Caswell J. L., Batchelor R. A., Forster J. R., Wellington K. J., 1989, Australian J. Phys., 42, 331
Caswell J. L., Vaile R. A., Ellingsen S. P., Whiteoak J. B., Norris R. P., 1995, MNRAS, 272, 96
Caswell J. L. et al., 2010, MNRAS, 404, 1029
Cragg D. M., Sobolev A. M., Godfrey P. D., 2002, MNRAS, 331, 521
Ellingsen S. P., von Bibra M. L., McCulloch P. M., Norris R. P., Deshpande A. A., Phillips C. J., 1996, MNRAS, 280 378
Felli M. et al., 2007, A&A, 476, 373
Forster J. R., Caswell J. L., 1989, A&A, 213, 339
Forster J. R., Caswell J. L., 1999, A&AS, 137, 43
Furuya R. S., Kitimara Y., Wootten A., Claussen M., Kawabe R., 2003, ApJS, 144, 71
Green J. A. et al., 2009, MNRAS, 392, 783
Matthews H. E., Olnon F. M., Winnberg A., Baud B., 1985, A&A, 149, 227
Minier V., Ellingsen S. P., Norris R. P., Booth R. S., 2003, A&A, 403, 1095
Palagi F., Cesaroni R., Comoretto G., Felli M., Natale V., 1993, A&AS, 101, 153
Walsh A. J., Lo N., Burton M. G., White G. L., Purcell C. R., Longmore S. N., Phillips C. J., Brooks K. J., 2008, Publ. Astron. Soc. Australia, 25, 105

This paper has been typeset from a TEX/LATEX file prepared by the author.